

RESEARCH

Open Access



Green synthesis, characterization, in silico molecular docking and biological evaluation of imidazolylchalcones as promising fungicide/s and nematicide/s

Rakesh Kumar^{1,2,3}, Parshant Kaushik¹, Kailashpati Tripathi^{1,4}, Rajni Godara¹, Sameer Ranjan Misra¹, Vijay Kumar¹, Partha Chandra Mondal¹, Jeetram¹, Pankaj⁵, Virendra Singh Rana¹, V. Shanmugam⁶, Dilip Khatri⁷ and Najam Akhtar Shakil^{1*}

Abstract

Chalcones are known for their broad biological activities, which can be enhanced by incorporating heterocyclic moieties. Imidazole, recognized for its diverse properties, was introduced into a series of imidazolylchalcone derivatives (3a–3o) synthesized via Claisen-Schmidt condensation of benzaldehydes (2a–2o) and 4-(imidazol-1-yl) acetophenone (1a) using ultrasonication as a green method. These compounds were characterized by spectroscopic techniques such as ¹H-NMR, ¹³C-NMR, LC-HRMS and evaluated for fungicidal and nematocidal activity. Compound 3h showed highest fungicidal activity against *Rhizoctonia solani* (ED₅₀ = 0.69 µg/mL), outperforming commercial hexaconazole (ED₅₀ = 3.57 µg/mL). Compound 3d exhibited the highest activity against *Fusarium oxysporum* (ED₅₀ = 119.22 µg/mL), while 3f was most effective against *Meloidogyne incognita* (LC₅₀ = 33.62 µg/mL), though less active than commercial Velum Prime (LC₅₀ = 3.46 µg/mL). The compounds potential activity may results from interactions of electronegative atom with enzyme active sites via hydrogen bonding. Docking studies against fungal cutinase and nematode acetylcholinesterase supported the in-vitro findings. Promising compounds will undergo further in-vivo and field trials for antifungal and antinemic applications and developed a potent molecule.

Keywords Green synthesis, Imidazolylchalcones, Ultrasonication, Molecular docking, *Fusarium oxysporum*, *Rhizoctonia solani*, *Meloidogyne incognita*

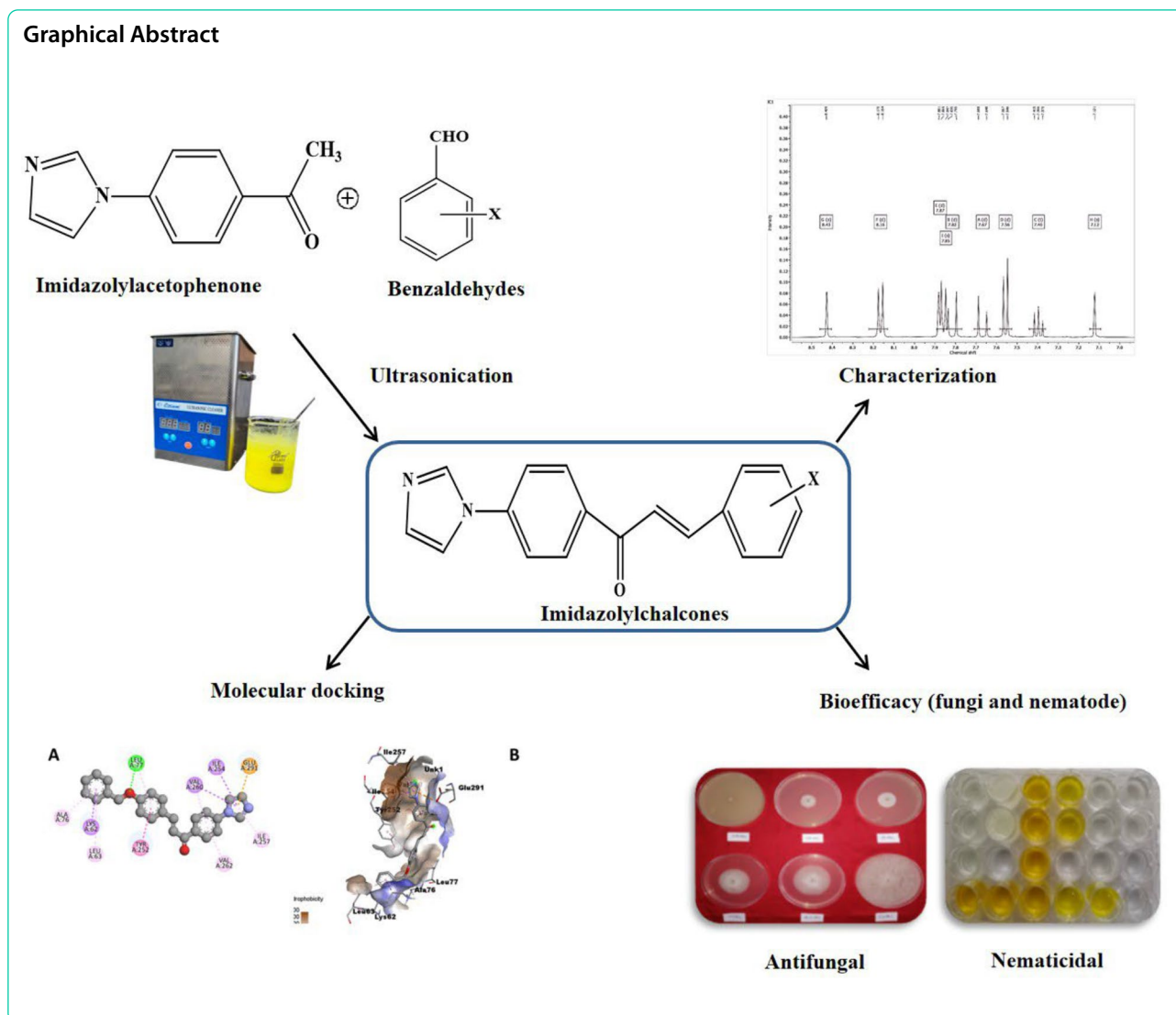
*Correspondence:

Najam Akhtar Shakil
iamshakil@gmail.com

Full list of author information is available at the end of the article



© The Author(s) 2025. **Open Access** This article is licensed under a Creative Commons Attribution-NonCommercial-NoDerivatives 4.0 International License, which permits any non-commercial use, sharing, distribution and reproduction in any medium or format, as long as you give appropriate credit to the original author(s) and the source, provide a link to the Creative Commons licence, and indicate if you modified the licensed material. You do not have permission under this licence to share adapted material derived from this article or parts of it. The images or other third party material in this article are included in the article's Creative Commons licence, unless indicated otherwise in a credit line to the material. If material is not included in the article's Creative Commons licence and your intended use is not permitted by statutory regulation or exceeds the permitted use, you will need to obtain permission directly from the copyright holder. To view a copy of this licence, visit <http://creativecommons.org/licenses/by-nc-nd/4.0/>.



Introduction

In modern agriculture, emerging diseases caused by fungi, bacteria, viruses, and nematodes pose a severe threat to global crop production, affecting yield and quality. Trade globalization and climate change have accelerated the spread of these infections, intensifying the challenge to food security and economic stability, especially in agriculture-dependent regions of world [1]. Pests and pathogens destroy 40–50% of crop yields, with plant diseases responsible for about a quarter of these losses [2] and plant parasitic nematodes cause an estimated 12.3% annual yield loss in global food production, valued at \$157 billion [3]. In the different food crops, vegetables are essential to a balanced human diet and play a crucial role in ensuring global nutritional security by supplying vital nutrients, vitamins, and minerals [4]. Vegetable crops were also highly affected by the most devastating

diseases include root rot, damping-off, charcoal rot, and wilt, are caused by pathogens like *Rhizoctonia solani*, *Alternaria solani*, *Fusarium oxysporum*, *Sclerotium rolfsii*, *Macrophomina phaseolina*, and *Pythium* spp. [5]. Among vegetables, *Solanum melongena* (brinjal) is a warm-season vegetable grown globally for its edible fruits and rich nutritional content. It provides essential nutrients such as dietary fiber, folate, vitamin C, vitamin K, niacin, vitamin B6, pantothenic acid, potassium, iron, magnesium, manganese, phosphorus, and copper [6]. Brinjal is also vulnerable to a range of biotic stresses includes pre- and post-emergence damping-off, root rot (*R. solani*), wilt (*F. oxysporum*) of seedlings at nursery stage and later by *Meloidogyne incognita* (Root-knot nematode) causes severe damage [7]. These soil-borne fungi and nematode cause severe plant mortality with significant crop losses of brinjal crops, which impacts

food security and livelihoods of large numbers of farmers' [8]. In case of high disease severity losses can escalate up to 25–75% [9] and 21% by nematode that may varied with host variety and environmental factors [10]. Therefore, losses caused by disease and insect infestation in brinjal must be managed to ensure proper growth and flourishing of the crop to meet demands. Over the past three decades, natural products from diverse microbial sources and botanicals have been explored for control of pests and diseases. However, due to narrow spectrum, low stability and low efficacy are limitation for immediate control of pests [11]. Although, synthetic pesticides have also shown limitations, such as health risks, pesticide residues, environmental impact, and the emergence of resistant pathogens. Additionally, climate change has affected the efficacy of these chemicals [12]. To overcome resistance, there is a need to synthesize safe, broad spectrum, efficient, cost-effective and potential bioactive molecule/s to control pests and diseases [13].

In recent years, there has been growing interest in heterocyclic compounds such as triazine [14], triazole [15, 16], tetrazole [17], benzimidazole [18, 19], thiadiazole [20–22], thiosemicarbazone [23], pyrrole [21, 22], imidazole [24], imidazothiazole [25], *bis*-Schiff base [26], oxadiazole [18, 19] and hybrid chalcone [27] etc., due to their wide range of bioactivity and have broad spectrum or multiple biological properties in medicinal chemistry. Among these, chalcones, a class of naturally occurring flavonoids, have emerged as potent bioactive molecules with a wide range of biological activities, including antifungal, antiparasitic, antibacterial, insecticidal, nematicidal, antioxidant, antiplasmodial, antitumor, and anthelmintic activities [28–30]. The structural diversity of chalcones and their ease of modification make them attractive candidates for the development of new agrochemicals [31]. Chalcones are α,β -unsaturated ketones characterized by the presence of two aromatic rings connected by a three-carbon α,β -unsaturated carbonyl system. This unique structure enables chalcones to exhibit various mechanisms of action, including enzyme inhibition, cell membrane disruption, and the generation of reactive oxygen species [32]. Furthermore, the introduction of heterocyclic moieties into the chalcone framework has been shown to enhance their biological activity [33, 34]. In this context imidazole, a five-membered heterocycle containing two nitrogen atoms, is one such moiety that has attracted significant attention due to its presence in a wide range of biologically active compounds [35]. Imidazole derivatives are known for their antibacterial, anti-inflammatory, antidiabetic, antiparasitic, antituberculosis, antifungal, antioxidant, antitumor, antimalarial, anticancer, antimicrobial and antidepressant properties [36–39] making them ideal candidates

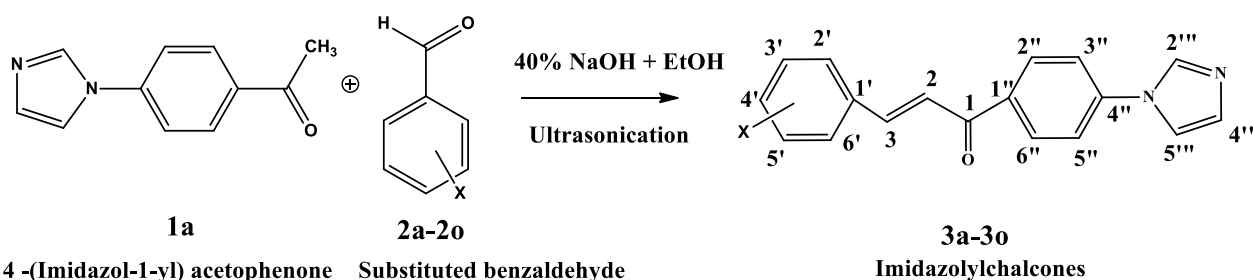
for the development of new agrochemicals or therapeutic agents.

In this context, imidazolylchalcones, a class of chalcones with an imidazole ring, can represent a promising avenue for the development of novel agrochemical. The introduction of the imidazole ring into the chalcone structure is expected to enhance the biological activity of the resulting compounds by improving their ability to interact with biological targets. Conventionally chalcone scaffold were synthesized via stirring of reagents in presence of alkali at room temperature with or without catalyst but in recent years, scientists are continuously working in environment friendly catalyst free synthesis of organic compounds. Notably, ultrasound-assisted organic synthesis has shown promise in achieving catalyst-free organic synthesis [40]. Ultrasonication has gained significant interest with a focus on multicomponent reactions at ambient reaction conditions, eco-friendly solvents and catalyst-free synthesis of bioactive heterocyclic scaffolds [41, 42]. Ultrasonic irradiation of the reaction mixture creates numerous cavitation bubbles that rapidly expand and then collapse intensely. This collapse generates micro-jets, facilitating the formation of a fine emulsion between the reactants [43]. Additionally, the violent implosions of these bubbles elevate the local temperature within the mixture, ultimately helping to overcome the activation energy barrier [44]. In this study, we report an eco-friendly synthesis of imidazolylchalcone derivatives via Claisen-Schmidt condensation using ultrasonication and compared with conventional synthetic approach, followed by evaluation against plant pathogenic fungi, *F. oxysporum*, *R. solani* and root knot nematode, *M. incognita*. Simultaneously, we carried out a computational modelling or docking study by simulating the binding of imidazolylchalcones to key enzymes, such as fungal cutinase and nematode acetylcholinesterase (AChE) to predict/identify lead compounds with high binding affinity and potential for biological efficacy. The potent compound/s in this series can be used as antifungal and antinemic agents to control soil-borne diseases and combat resistance in insect pests against commercial agrochemicals.

Materials and methods

Chemicals and instruments

Benzaldehydes, 4-(Imidazol-1-yl) acetophenone ($\geq 95.55\%$ purity) were obtained from Sigma-Aldrich and used without further purification. Analytical grade solvents and chemicals were used. Thin layer chromatography (TLC) was used to monitor reactions on 200 mm thick aluminium sheets of Merck silica gel 60F₂₅₄ and spots were visualised under UV light. A Heidolf rotary evaporator was employed for solvent removal. ¹H-NMR



X = **2a**: 2,6-Cl, **2b**: 4-F, **2c**: 4-Br, **2d**: 2-Br, **2e**: 2-NO₂, **2f**: 3-NO₂, **2g**: 4-NO₂, **2h**: 4-OCH₂-C₆H₅, **2i**: 4-OCH₃, **2j**: 3-Cl, **2k**: 2,4-Cl, **2l**: 2-Cl, **2m**: 3-OH, **2n**: 4-OH, **2o**: 3,4,5-OCH₃

Scheme 1 General method for the synthesis of Imidazolylchalcones

and ¹³C-NMR spectra were obtained on a JEOL 400 MHz Spectrospin spectrometer, with tetramethylsilane (TMS) serving as an internal standard for calibration. Liquid Chromatography-High Resolution Mass Spectrometry (LC-HRMS) was performed using an AB SCIEX Triple TOFTM 5600+ apparatus with TurboIonSpray (TIS), SCIEX ExionLC, and a PDA detector. A C₁₈ column (2.7 μm, 4.6 × 100 mm) was utilised for compound separation. The column was eluted with Methanol: Water (98:2% (v/v) containing 0.1% formic acid at a flow rate of 1.0 mL/min and a column oven temperature of 40 °C. Ultrasonic bath (Labman Scientific Instruments) was used for synthesis and cleaning of glasswares. Melting point was recorded in Buchi M-560 instrument and were uncorrected.

Methods of synthesis

Conventional synthesis of imidazolylchalcones (single step reaction)

The imidazolyl chalcone series was synthesized via base-catalyzed Claisen-Schmidt reaction [45]. Equimolar (1:1) amounts of selected benzaldehydes were dissolved in 5 mL of 40% ethanolic NaOH solution in a round-bottomed flask and stirred at room temperature for 10 min. After that, 4-(Imidazol-1-yl) acetophenone (dissolved in 5 mL of ethanol) was added dropwise with continuously stirring on magnetic stirrer. The stirring duration ranged from 1 to 28 h for different reactions at room temperature, as shown in Scheme 1. After the reaction was complete, the reaction mixture was neutralized with 2 M HCl, resulting in the formation of a creamy white or light-yellow precipitate. This precipitate was separated by filtration and rinsed with cold water. In case of no precipitate formation, the reaction mixture was extracted with ethyl acetate (30 mL × 3). The organic layer was dehydrated using anhydrous Na₂SO₄ and solvent was removed using a rotary evaporator, leaving behind a viscous residue.

Ultrasonic synthesis of imidazolylchalcones (single step reaction)

Equimolar amounts (1:1) of 4-(Imidazol-1-yl) acetophenone (100 mg, 0.537 mmol) in 40% ethanolic KOH (5 mL) was taken in 250 mL round bottom flask and ethanolic solution of the different benzaldehydes were added. RB flask was fixed with burette stand in ultrasonic bath at temp. 25–30 °C, frequency 40 kHz with time range, 5–90 min., depending on the compounds listed in Scheme 1 and the reactions were monitored by TLC in ethyl acetate: hexane (2:8) solvent systems. After completion of reaction, reaction mixture was worked up as described in conventional method. Out of all synthesized compounds, few were crystallized in methanol without further purification and few were purified through column chromatography by gradient increasing in the polarity of mobile phase/solvent. Column started with pure hexane and gradually increased polarity with the ethylacetate combination and pure compound comes in the range of 7–10% ethylacetate in the hexane. 50 mL fractions were collected and monitored with TLC.

Spectral analysis of imidazolylchalcone derivatives

(E)-1-(4-(1H-imidazole-1-yl) phenyl)-3-(2,6-dichlorophenyl) prop-2-en-1-one (3a)

Creamy yellow solid; m.p.: 149–151 °C, R_f: 0.56 (Hexane: ethyl acetate, 1:4). ¹H NMR (400 MHz, DMSO-*d*₆) δ 8.28 (1H, d, J = 16.8 Hz, H-3), 8.02–7.92 (3H, m, Ar-H'), 7.89 (1H, d, J = 16.8 Hz, H-2), 7.84–7.63 (4H, m, Ar-H''), 7.37–7.20 (2H, m, H-4''' & H-5'''), 7.11 (1H, s, H-2'''). ¹³C NMR (101 MHz, DMSO-D₆) δ 198.01 (C1), 143.54 (C3), 140.76 (C4''), 136.26 (C1'''), 135.07 (C1'; C2'''), 131.90 (C2'; C6'), 130.94 (C2''; C3''; C5''; C6''), 130.45 (C4'''), 128.22 (C3'; C5'), 126.38 (C4'), 120.20 (C2), 118.29 (C5'''). HRMS for C₁₈H₁₂Cl₂N₂O [M+H]⁺ m/z: Calcd 343.0394; Observed 343.0399.

(E)-1-(4-(1H-imidazole-1-yl)phenyl)-3-(4-fluorophenyl)**prop-2-en-1-one (3b)**

Yellow-brown solid; m.p.: 144–145 °C, R_f : 0.55 (Hexane: ethyl acetate, 1:4). ^1H NMR (400 MHz, DMSO- d_6) δ 8.35 (1H, d, $J=16.7$ Hz, H-3), 8.28–8.09 (4H, m, Ar-H $''$), 7.94 (1H, d, $J=16.7$ Hz, H-2), 7.63–7.40 (6H, m, Ar-H' & H-4 $''$, H-5 $''$), 7.16 (1H, s, H-2 $''$). ^{13}C NMR (101 MHz, DMSO- D_6) δ 189.70 (C-1), 162.15 (FC, d, $j=245$ Hz, C-4'), 143.65 (C-3), 142.83 (C-4 $''$), 137.49 (C-1 $''$), 135.60 (C-2 $''$), 130.70 (C-2', C-6'), 130.40 (FCmeta, $J=8.1$ Hz, C-2', C-3', C-5', C-6 $''$), 129.93 (FCpara $J=2$ Hz, C-1'), 129.48 (C-4 $''$), 121.30 (C-2), 118.20 (C-5 $''$), 115.40 (FCortho, $J=22$ Hz, C-3', C-5'). HRMS for $\text{C}_{18}\text{H}_{13}\text{FN}_2\text{O}$ $[\text{M}+\text{H}]^+m/z$: Calcd 293.1084; Observed 293.1085.

(E)-1-(4-(1H-imidazole-1-yl)phenyl)-3-(4-bromophenyl)**prop-2-en-1-one (3c)**

White solid; m.p.: 161–162 °C, R_f : 0.57 (Hexane: ethyl acetate, 1:4). ^1H NMR (400 MHz, DMSO- d_6) δ 8.02 (1H, d, $J=15.7$ Hz, H-3), 7.96–7.77 (8H, m, Ar-H' & Ar-H $''$), 7.70 (1H, d, $J=15.7$ Hz, H-2), 7.66–7.59 (2H, m, H-4 $''$ & H-5 $''$), 7.13 (1H, s, H-2 $''$). ^{13}C NMR (101 MHz, DMSO- d_6) δ 188.22 (C-1), 143.37 (C-3), 140.86 (C-4 $''$), 136.32 (C-1 $''$), 135.85 (C-2 $''$), 134.49 (C-1'), 132.42 (C-3'), 132.42 (C-5'), 131.45 (C-2 $''$), 131.45 (C-6 $''$), 131.13 (C-3 $''$), 131.13 (C-5 $''$), 130.95 (C-4 $''$), 128.52 (C-2'), 128.52 (C-6'), 123.08 (C-4'), 120.31 (C-2), 118.35 (C-5 $''$). HRMS for $\text{C}_{18}\text{H}_{13}\text{BrN}_2\text{O}$ $[\text{M}+\text{H}]^+m/z$: Calcd 353.0311; Observed 353.0284.

(E)-1-(4-(1H-imidazole-1-yl)phenyl)-3-(2-bromophenyl)**prop-2-en-1-one (3d)**

Cream yellow solid; m.p.: 121–123 °C, R_f : 0.70 (Hexane: ethyl acetate, 1:4). ^1H NMR (400 MHz, DMSO- d_6) δ 8.29 (1H, d, $J=16.9$ Hz, H-3), 8.24–8.01 (4H, m, Ar-H $''$), 7.89 (4H, d, $J=16.9$ Hz, H-2), 7.86–7.67 (4H, m, Ar-H'), 7.56–7.24 (2H, m, H-4 $''$ & H-5 $''$), 7.13 (1H, s, H-2 $''$). ^{13}C NMR (101 MHz, DMSO- d_6) δ 188.12 (C-1), 141.95 (C-3), 140.98 (C-4 $''$), 136.34 (C-1 $''$), 135.65 (C-2 $''$), 133.85 (C-1'), 132.82 (C-3'), 131.23 (C-2', C-6 $''$), 130.98 (C-3', C-5 $''$), 129.42 (C-4 $''$), 128.77 (C-6'), 126.03 (C-5'), 125.16 (C-4'), 120.32 (C-2'), 120.15 (C-2), 118.33 (C-5 $''$). HRMS for $\text{C}_{18}\text{H}_{13}\text{BrN}_2\text{O}$ $[\text{M}+\text{H}]^+m/z$: Calcd 353.0311; Observed 353.0284.

(E)-1-(4-(1H-imidazole-1-yl)phenyl)-3-(2-nitrophenyl)**prop-2-en-1-one (3e)**

Black solid; m.p.: 118–120 °C, R_f : 0.56 (Hexane: ethyl acetate, 1:4). ^1H NMR (400 MHz, DMSO- d_6) δ 8.45 (1H, d, $J=15.4$ Hz, H-3), 8.42–8.34 (4H, m, Ar-H $''$), 8.18 (1H, d, $J=15.4$ Hz, H-2), 8.12–7.67 (6H, m, Ar-H' & H-4 $''$, H-5 $''$), 7.12 (1H, s, H-2 $''$). ^{13}C NMR (101 MHz, DMSO- d_6) δ 203.51 (C-1), 147.95 (C-2'), 145.67 (C-3), 143.48 (C-4 $''$),

137.87 (C-1 $''$), 136.12 (C-2 $''$), 134.70 (C-5'), 131.74 (C-2', C-3', C-5', C-6 $''$), 130.65 (C-4 $''$), 129.19 (C-4'), 128.37 (C-1'), 126.87 (C-6'), 123.96 (C-3'), 120.85 (C-2), 118.39 (C-5 $''$). HRMS for $\text{C}_{18}\text{H}_{13}\text{N}_3\text{O}_3$ $[\text{M}+\text{H}]^+m/z$: Calcd 320.1027; Observed 320.1030.

(E)-1-(4-(1H-imidazole-1-yl)phenyl)-3-(3-nitrophenyl)**prop-2-en-1-one (3f)**

Pale-yellow solid; m.p.: 141–143 °C, R_f : 0.54 (Hexane: ethyl acetate, 1:4). ^1H NMR (400 MHz, DMSO- d_6) δ 8.44 (1H, s, H-2'), 8.26 (1H, d, $J=15.5$ Hz, H-3), 7.95–7.85 (3H, m, H-4', H-5', H-6'), 7.84 (1H, d, $J=15.5$ Hz, H-2), 7.35–7.16 (6H, m, Ar-H $''$ & H-4 $''$, H-5 $''$), 7.13 (1H, s, H-2 $''$). ^{13}C NMR (101 MHz, DMSO- d_6) δ 197.74 (C-1), 148.22 (C-3'), 142.58 (C-4 $''$), 140.84 (C-3), 136.26 (C-1'), 136.26 (C-1 $''$), 135.52 (C-2 $''$), 134.97 (C-6'), 130.94 (C-2 $''$), 130.94 (C-6 $''$), 130.47 (C-3 $''$), 130.47 (C-5 $''$), 130.47 (C-4 $''$), 128.16 (C-5'), 123.12 (C-4'), 120.19 (C-2'), 120.19 (C-2), 118.28 (C-5 $''$). HRMS for $\text{C}_{18}\text{H}_{13}\text{N}_3\text{O}_3$ $[\text{M}+\text{H}]^+m/z$: Calcd 320.1027; Observed 320.1030.

(E)-1-(4-(1H-imidazole-1-yl)phenyl)-3-(4-nitrophenyl)**prop-2-en-1-one (3g)**

Light brown solid; m.p.: 165–167 °C, R_f : 0.59 (Hexane: ethyl acetate, 1:4). ^1H NMR (400 MHz, DMSO- d_6) δ 8.25 (1H, d, $J=16.4$ Hz, H-3), 8.15–8.00 (4H, m, Ar-H $''$), 7.91–7.77 (4H, m, Ar-H $''$), 7.64 (1H, d, $J=16.4$ Hz, H-2), 7.57–7.41 (2H, m, H-4 $''$ & H-5 $''$), 7.16 (1H, s, H-2 $''$). ^{13}C NMR (101 MHz, DMSO- d_6) δ 201.17 (C-1), 151.76 (C-4'), 147.01 (C-3), 143.84 (C-4 $''$), 142.11 (C-1'), 136.03 (C-1 $''$), 134.89 (C-2 $''$), 131.25 (C-2', C-3', C-5', C-6 $''$), 130.43 (C-4 $''$), 128.16 (C-2', C-6'), 123.83 (C-3', C-5'), 120.89 (C-2), 118.89 (C-5 $''$). HRMS for $\text{C}_{18}\text{H}_{13}\text{N}_3\text{O}_3$ $[\text{M}+\text{H}]^+m/z$: Calcd 320.1027; Observed 320.1030.

(E)-1-(4-(1H-imidazole-1-yl)phenyl)-3-(4-(benzyloxy)**phenyl)prop-2-en-1-one (3h)**

Cream white solid; m.p.: 153–155 °C, R_f : 0.70 (Hexane: ethyl acetate, 1:4). ^1H NMR (400 MHz, DMSO- d_6) δ 8.25 (1H, d, $J=15.9$ Hz, H-3), 7.91–7.81 (4H, m, Ar-H $''$), 7.47–7.39 (2H, m, H-4 $''$ & H-5 $''$), 7.39–7.25 (9H, m, Ar-H' & Ar-Ha'), 7.13 (1H, s, H-2 $''$), 7.07 (1H, d, $J=15.9$ Hz, H-2), 5.15 (2H, s, $-\text{OCH}_2$). ^{13}C NMR (101 MHz, DMSO- d_6) δ 188.14 (C-1), 161.04 (C-4'), 144.71 (C-3), 140.64 (C-4 $''$), 137.20 (C-1 $''$), 136.30 (C-1'a), 136.26 (C-2 $''$), 131.48 (C-2', C-6 $''$), 130.93 (C-3', C-5 $''$), 129.02 (C-2', C-6'), 128.51 (C-4 $''$), 128.35 (C-3'a, C-5'a), 128.03 (C-4'a, C-1'), 127.25 (C-2'a, C-6'a), 120.28 (C-2), 118.34 (C-5 $''$), 115.76 (C-3', C-5'), 69.92 (OCH_2). HRMS for $\text{C}_{25}\text{H}_{20}\text{N}_2\text{O}_2$ $[\text{M}+\text{H}]^+m/z$: Calcd 381.1462; Observed 381.1468.

(E)-1-(4-(1H-imidazole-1-yl)phenyl)-3-(4-methoxyphenyl)prop-2-en-1-one (3i)

Cream white solid; m.p.: 146–147 °C, R_f : 0.57 (Hexane: ethyl acetate, 1:4). ^1H NMR (400 MHz, DMSO- d_6) δ 8.26 (1H, d, $J=16.4$ Hz, H-3), 7.97–7.62 (10H, m, Ar-H', Ar-H'' & H-4'', H-5'''), 7.13 (1H, s, H-2'''), 6.98 (1H, d, $J=16.4$ Hz, H-2), 3.78 (3H, s, OCH₃). ^{13}C NMR (101 MHz, DMSO- d_6) δ 188.15 (C-1), 161.97 (C-4'), 144.78 (C-3), 140.63 (C-4''), 136.27 (C-1'''), 135.12 (C-2'''), 131.49 (C-2'', C-3'', C-5'', C-6''), 130.92 (C-2', C-6', C-4'''), 127.83 (C-1'), 120.28 (C-2), 118.34 (C-5'''), 114.94 (C-3', C-5'), 55.93 (–OCH₃). HRMS for C₁₉H₁₆N₂O₂ [M+H]⁺ m/z : Calcd 305.1314; Observed 305.1318.

(E)-1-(4-(1H-imidazole-1-yl)phenyl)-3-(3-chlorophenyl)prop-2-en-1-one (3j)

Pale-yellow solid; m.p.: 142–143 °C, R_f : 0.56 (Hexane: ethyl acetate, 1:4). ^1H NMR (400 MHz, DMSO- d_6) δ 8.26 (1H, d, $J=16.9$ Hz, H-3), 7.94–7.86 (4H, m, Ar-H''), 7.83 (1H, d, $J=16.9$ Hz, H-2), 7.33–7.17 (6H, m, Ar-H' & H-4'', H-5'''), 7.13 (1H, s, H-2'''). ^{13}C NMR (101 MHz, DMSO- d_6) δ 188.14 (C-1), 145.87 (C-3), 140.98 (C-4''), 139.19 (C-1'''), 136.34 (C-1'), 135.65 (C-2'''), 134.98 (C-3'), 132.66 (C-2'', C-6''), 131.23 (C-3'', C-5''), 130.97 (C-4'''), 130.58 (C-5'), 129.25 (C-4'), 128.24 (C-6'), 125.02 (C-2'), 120.33 (C-2), 118.34 (C-5'''). HRMS for C₁₈H₁₃ClN₂O [M+H]⁺ m/z : Calcd 309.0784; Observed 309.0789.

(E)-1-(4-(1H-imidazole-1-yl)phenyl)-3-(2,4-dichlorophenyl)prop-2-en-1-one (3k)

Brown solid; m.p.: 125–126 °C, R_f : 0.55 (Hexane: ethyl acetate, 1:4). ^1H NMR (400 MHz, DMSO- d_6) δ 8.03 (1H, d, $J=16.2$ Hz, H-3), 7.86 (1H, s, H-3'), 7.80 (1H, d, $J=16.2$ Hz, H-2), 7.75–7.65 (6H, m, Ar-H'' & H-4'', H-5'''), 7.52 (1H, d, $J=2.1$ Hz, H-5'), 7.50 (1H, d, $J=2.1$ Hz, H-6'), 7.11 (1H, s, H-2'''). ^{13}C NMR (101 MHz, DMSO- d_6) δ 197.36 (C-1), 140.75 (C-3), 137.60 (C-4''), 136.78 (C-1'''), 136.26 (C-2'), 135.30 (C-2'''), 131.60 (C-1'), 130.64 (C-2'', C-3'', C-5'', C-6''), 130.58 (C-6', C-4'''), 128.13 (C-3'), 126.58 (C-5'), 125.38 (C-4'), 120.19 (C-2), 118.30 (C-5'''). HRMS for C₁₈H₁₂Cl₂N₂O [M+H]⁺ m/z : Calcd 344.0232; Observed 344.0238.

(E)-1-(4-(1H-imidazole-1-yl)phenyl)-3-(2-chlorophenyl)prop-2-en-1-one (3l)

Pale-yellow solid; m.p.: 114–116 °C, R_f : 0.54 (Hexane: ethyl acetate, 1:4). ^1H NMR (400 MHz, DMSO- d_6) δ 8.29 (1H, d, $J=16.4$ Hz, H-3), 8.10–8.01 (4H, m, Ar-H''), 7.87 (1H, d, $J=16.4$ Hz, H-2), 7.58–7.50 (2H, m, H-4'' & H-5'''), 7.49–7.37 (4H, m, Ar-H'), 7.13 (1H, s, H-2'''). ^{13}C NMR (101 MHz, DMSO- d_6) δ 188.14 (C-1), 140.98 (C-3), 139.19 (C-4''), 136.34 (C-1'''), 135.65 (C-2'''), 134.97 (C-2'), 132.66 (C-1'), 131.23 (C-2'', C-3'', C-5'', C-6''),

130.97 (C-4'''), 130.58 (C-3'), 129.25 (C-4'), 128.24 (C-6'), 125.02 (C-5'), 120.33 (C-2), 118.34 (C-5'''). HRMS for C₁₈H₁₃ClN₂O [M+H]⁺ m/z : Calcd 309.0784; Observed 309.0789.

(E)-1-(4-(1H-imidazole-1-yl)phenyl)-3-(3-hydroxyphenyl)prop-2-en-1-one (3m)

Cream white solid; m.p.: 232–234 °C, R_f : 0.57 (Hexane: ethyl acetate, 1:4). ^1H NMR (400 MHz, DMSO- d_6) δ 8.26 (1H, d, $J=15.8$ Hz, H-3), 7.96–7.87 (4H, m, Ar-H''), 7.84 (1H, d, $J=15.8$ Hz, H-2), 7.37–7.15 (5H, m, H-4', H-5', H-6' & H-4'', H-5'''), 7.13 (1H, s, H-2'''), 6.86 (1H, s, H-2'), 5.41 (1H, s, –OH). ^{13}C NMR (101 MHz, DMSO- d_6) δ 188.37 (C-1), 158.40 (C-3'), 145.07 (C-3), 140.75 (C-4''), 136.44 (C-1'''), 136.31 (C-1'), 136.03 (C-2'''), 131.05 (C-2'', C-3'', C-5'', C-6''), 130.93 (C-5'), 130.41 (C-4'''), 122.15 (C-2), 120.32 (C-6'), 118.48 (C-5'''), 118.34 (C-2'), 115.95 (C-4'). HRMS for C₁₈H₁₄N₂O₂ [M+H]⁺ m/z : Calcd 291.0632; Observed 291.0628.

(E)-1-(4-(1H-imidazole-1-yl)phenyl)-3-(4-hydroxyphenyl)prop-2-en-1-one (3n)

Cream yellow solid; m.p.: 247–249 °C, R_f : 0.55 (Hexane: ethyl acetate, 1:4). ^1H NMR (400 MHz, DMSO- d_6) δ 8.34 (1H, d, $J=15.8$ Hz, H-3), 8.18–7.98 (4H, m, Ar-H''), 7.98–7.77 (6H, m, Ar-H' & H-4'', H-5'''), 7.73 (1H, d, $J=15.8$ Hz, H-2), 7.16 (1H, s, H-2'''), 5.57 (1H, s, –OH). ^{13}C NMR (101 MHz, DMSO- d_6) δ 197.62 (C-1), 157.58 (C-4'), 144.76 (C-3), 138.79 (C-4''), 137.40 (C-1'''), 135.38 (C-2'''), 130.51 (C-2'', C-3'', C-5'', C-6''), 130.01 (C-4'''), 127.42 (C-1'), 122.28 (C-2), 118.47 (C-5'''), 115.80 (C-3', C-5'). HRMS for C₁₈H₁₄N₂O₂ [M+H]⁺ m/z : Calcd 291.0632; Observed 291.0628.

(E)-1-(4-(1H-imidazole-1-yl)phenyl)-3-(3,4,5-trimethoxyphenyl)prop-2-en-1-one (3o)

Yellow brown solid; m.p.: 135–137 °C, R_f : 0.56 (Hexane: ethyl acetate, 1:4). ^1H NMR (400 MHz, DMSO- d_6) δ 8.28 (1H, d, $J=16.8$ Hz, H-3), 7.88 (1H, d, $J=16.8$ Hz, H-2), 7.78–7.35 (6H, m, Ar-H'' & H-4'', H-5'''), 7.23 (2H, s, H-2' & H-6'), 7.14 (1H, s, H-2'''), 3.83 (9H, s, –OCH₃). ^{13}C NMR (101 MHz, DMSO- d_6) δ 188.33 (C-1), 153.63 (C-3', C-5'), 145.31 (C-3), 140.74 (C-4''), 140.31 (C-4'), 136.33 (C-1'''), 136.02 (C-2'''), 131.06 (C-2'', C-3'', C-5'', C-6''), 130.95 (C-4'''), 127.51 (C-1'), 120.32 (C-2), 118.36 (C-5'''), 107.16 (C-2', C-6'), 60.68 (4'-OCH₃), 56.66 (3'-OCH₃ & 5'-OCH₃). HRMS for C₂₁H₂₀N₂O₄ [M+H]⁺ m/z : Calcd 365.0839; Observed 365.0842.

Antifungal bioassay

Imidazolylchalcone derivatives were assessed for their antifungal properties in vitro against *R. solani* and *F. oxysporum* using the poisoned food technique [46]. The

fungal strains, *F. oxysporum* ITCC 8113 and *R. solani* ITCC 7479 were obtained from ITCC (Indian Type Culture Collection), Division of Plant Pathology, ICAR-IARI, New Delhi, India. These cultures were kept at 27 °C for 4–7 days on PDA (Potato Dextrose Agar) slants and were regularly subcultured to maintain their viability and purity.

The stock solution of synthesized compounds (1000 µg mL⁻¹) was prepared in DMSO. An in vitro bioassay was carried out at five different concentrations namely 200, 100, 50, 25 and 12.5 µg mL⁻¹ using freshly prepared PDA media in quadruplicate. Positive controls for *F. oxysporum* and *R. solani* were carbendazim 50% WP (Wettable Powder) and Hexaconazole 5% SC (Soluble Concentrate), respectively. Fungal spores and mycelium were taken from subcultured fungal cultures using a 5-mm-thick disc, which was then inoculated in Petri dishes under laminar flow (sterile conditions). The treatment and control Petri dishes were placed in a BOD incubator at 25 ± 1 °C. Incubation was continued until the fungal growth completely covered or reached an advanced stage in the control Petri dish, which usually took about 4–5 days for *R. solani* and 10–12 days for *F. oxysporum* [47]. Percentage inhibition was calculated by measuring colony diameter of fungi [48].

$$I = \{(C - T)/C\} \times 100$$

where, I represent inhibition percentage, C for mean diameter (cm) of growth of fungal colony in control and T for treated Petri dishes.

The corrected percentage inhibition (IC) was determined with the following equation:

$$IC = (I - CF)/(100 - CF) \times 100$$

Here, CF is calculated as:

$$CF = [(90 - C)/C] \times 100$$

where, 90 is Petri plate diameter (mm) and C represent fungal mycelial growth (mm) in control plate.

Nematicidal bioassay

M. incognita (root knot nematode) extracted from the infected root galls of brinjal nursery of Division of Nematology, ICAR-IARI, New Delhi. All synthesized compounds were evaluated for in vitro nematicidal activity using a water screening method. For extraction of nematode culture, galls were incubated at 25–30 °C for 2–3 days, which facilitate the hatching of eggs. Subsequently, nematode population counted and 100 J2s per mL was prepared through dilution.

Synthesized compound's stock solution of 1000 µg mL⁻¹ was prepared in DMSO. The five test

concentrations (200, 100, 50, 25 and 12.5 µg mL⁻¹) were prepared through serial dilution from stock solution. Velum prime was taken as positive control for *M. incognita*. A 1 mL suspension of nematodes (J2s) with 1 mL of test compound of different concentrations were added into 24-well culture plates and incubated at 28 ± 2 °C in BOD in triplicates. Both living and dead J2s nematodes were counted in each treatment using a counting dish under stereoscopic binocular microscope. The mortality of J2s nematodes was recorded at 24, 48, 72 and 96 h [49–51]. The mortality rate was determined by Abbott's formula [48].

$$\begin{aligned} &\text{Corrected mortality percentage} \\ &= [(T - C)/(100 - C)] \times 100 \end{aligned}$$

Here, T and C represents total mortality in the treatment and control, respectively.

ED₅₀ values (effective dose for 50% inhibition) for antifungal and LC₅₀ values (lethal concentration for 50% inhibition) for nematicidal activities were expressed in µg mL⁻¹, computed by probit analysis using the SPSS statistical package (version 28.0).

Molecular docking

Molecular docking is an essential tool for drug and agrochemical discovery, helping in virtual screening of potential candidates as well as providing insights into the mechanism of action of a certain compound [52]. In this study, cutinase and elongation factor proteins were selected as targets for the fungicidal activity whereas acetylcholinesterase was chosen as a target site for nematicidal action. Cutinase and elongation factor both play a crucial role in growth, survival, and virulence of both the fungi. Hence, these enzymes are a potential target for developing new antifungal agents. Similarly, acetylcholinesterase is one of the most important enzyme responsible for maintaining steady transfer of nerve signal, making it a potential target site for various pests including nematodes [32]. The target enzyme sequences were obtained from the NCBI database (<https://www.ncbi.nlm.nih.gov/>) and used for homology modeling with the SWISS-MODEL tool (<https://swissmodel.expasy.org/>). FASTA codes of the target sequence, retrieved from the NCBI database, were used to search for templates for the homology modelling. The templates were chosen based on coverage and GMQE (Global Model Quality Estimate). Homology modeling is a method that constructs a three-dimensional protein structure from a target protein sequence, using the three-dimensional structure of a homologous protein as a template. In situations where the crystal structure of a protein is not available, a homology model may be employed as an alternative approach

for receptor-ligand analyses such as molecular docking, given the existence of a three-dimensional structure of a related protein [53]. The details regarding the homology modelling are illustrated in Table 1. Protein and ligand preparation was conducted using AutoDock tools. For protein preparation, water molecules were removed, polar hydrogens were added, and appropriate charges were assigned. The two-dimensional structures of the ligand compounds were initially created using ChemDraw Ultra 12.0, and subsequently converted to three-dimensional structures using Chem3D Pro 12.0, followed by energy minimization. These structures were then saved in pdb format using PyMOL and further processed for molecular docking in AutoDock tools. Following the docking simulations, ligands were ranked based on their binding affinities. Detailed analyses of the most favorable ligand-protein interactions were performed using BIOVIA Discovery Studio.

Results and discussion

Synthesis and characterization

Fifteen imidazolylchalcone derivatives were synthesized successfully using both conventional and ultrasonic methods (Scheme 1). The ultrasonication method showed shorter reaction times and higher yields compared to the conventional approach (Table 2).

In imidazolylchalcones (**3a–3o**), two characteristic doublets of olefinic protons appeared at approximately 7.82 (1H, d, $J=15.9$ Hz, H-3) and 7.67 (1H, d, $J=15.9$ Hz, H-2) in the $^1\text{H-NMR}$ spectrum of all the compounds, confirming the formation of chalcones. In $^{13}\text{C-NMR}$, the peak at δ 188.14–203.51 (C-1) for the carbonyl moiety and peaks at δ 140.75–147.01 (C-3) and 120.15–122.28 (C-2) for the olefinic carbon atoms of imidazolylchalcone were observed. The multiplet present between δ 7.16–8.42 (4H, m, Ar-H') indicates the presence of a phenyl ring at the carbonyl carbon atom in the $^1\text{H-NMR}$ spectra of all the derivatives. A characteristic peak at 7.11–7.13 (H2'') and the multiplet between δ 7.15–8.12 (H3'' & H4'') confirmed the presence of imidazolyl ring. The multiplet appearing between δ 7.17 and 8.15 (Ar-H') showed the presence of a substituted phenyl ring connected to the C-3 carbon and the chemical shift of this

Table 2 Comparison of reaction time and yield of ultrasonic and conventional methods of imidazolylchalcones

Compounds	Conventional method		Ultrasonication method	
	Reaction time (min)	Yield (%)	Reaction time (min)	Yield (%)
3a	30	84	5	92
3b	130	79	40	91
3c	70	81	30	88
3d	25	80	5	87
3e	170	77	60	84
3f	230	72	70	85
3g	210	74	90	87
3h	120	81	40	89
3i	90	79	30	86
3j	110	76	50	84
3k	105	80	40	91
3l	60	85	20	91
3m	150	83	50	92
3n	170	84	60	89
3o	250	74	90	82

ring was influenced by different substituents like halo, nitro, hydroxy and methoxy groups. Characteristic singlets between δ 3.78 and 3.83 indicated the presence of methoxy groups in the compounds **3i** and **3o**. Similarly, compounds **3m** and **3n** showed characteristic singlet between 5.41 and 5.57, due to the presence of hydroxy group and compound **3h** showed characteristic singlet at 5.15 confirmed the benzyloxy ($-\text{OCH}_2-$) group. The structures of all the compounds were further confirmed by $^{13}\text{C-NMR}$ spectra, which matched well with the respective carbon atom values.

Antifungal activity

The in vitro results of antifungal activity of synthesized imidazolylchalcone derivatives against *R. solani* and *F. oxysporum* are presented in Tables 3 and 4. It showed that compound **3h** exhibited the most potent fungicidal activity, with an ED_{50} value of $0.69 \mu\text{g mL}^{-1}$, significantly lower than the ED_{50} value ($3.57 \mu\text{g mL}^{-1}$) of commercially available hexaconazole 5% SC fungicide

Table 1 Homology modeling parameters of the target proteins

Target pest	Target protein	Target sequence ID	Template protein PDB ID	GMQE
<i>Fusarium oxysporum</i>	Elongation factor	KAH7490335.1	6gfu.1.A	0.77
	Cutinase	KAJ9428189.1	1bs9.1.A	0.30
<i>Rhizoctonia solani</i>	Elongation factor	NP_776960.1	6ra9.1.B	0.90
	Cutinase	CCO31306.1	5ajh.1.A	0.56
<i>Meloidogyne incognita</i>	Acetylcholinesterase	AFJ54351.1	6ary.1.A	0.71

Table 3 in vitro antifungal potential of imidazolylchalcone derivatives against *Rhizoctonia solani*

Compounds	Regression equation	χ^2	ED ₅₀ ($\mu\text{g mL}^{-1}$)	Fiducial limit
3a	0.714X + - 1.714	2.31	410.3 ^h	208.3–1867.47
3b	1.143X + - 2.543	0.72	176.08 ^{gh}	124.86–301.5
3c	0.5X + - 0.5	0.17	8.48 ^{b-e}	0.35–19.64
3d	0.714X + - 0.714	0.007	8.81 ^{b-e}	2.80–15.44
3e	1.0X + - 1.8	0.15	14.84 ^{b-e}	8.39–21.22
3f	1.0X + - 1.8	9.56	32.71 ^{d-f}	1.17–86.56
3g	0.714X + - 0.514	0.27	4.35 ^{ab}	0.65–9.59
3h	0.571X + - 0.229	0.19	0.69 ^a	0.005–3.06
3i	0.429X + - 0.529	0.27	15.13 ^{b-f}	2.26–29.02
3j	0.5X + - 0.1	0.78	2.28 ^{a-c}	0.035–7.44
3k	0.714X + - 0.514	0.28	6.75 ^{a-d}	1.85–12.51
3l	1.0X + - 1.4	2.69	29.26 ^{c-f}	18.45–40.80
3m	0.357X + - 0.757	0.03	134.62 ^{fg}	63.53–3441.93
3n	0.571X + - 0.971	0.66	36.42 ^{ef}	19.31–57.81
3o	0.857X + - 1.257	2.34	22.66 ^{b-f}	13.37–32.01

* Hexaconazole 5% SC, ED₅₀ = 3.57 $\mu\text{g mL}^{-1}$ * ED₅₀ values with different superscripts are significantly different ($p < 0.001$)**Table 4** In vitro antifungal potential of imidazolylchalcone derivatives against *Fusarium oxysporum*

Compounds	Regression equation	χ^2	ED ₅₀ ($\mu\text{g mL}^{-1}$)	Fiducial limit
3a	0.86X + - 2.06	1.01	361.62 ^{a-d}	185.7–1664.54
3b	0.86X + - 2.46	0.34	1272.2 ^{c-f}	459.65–17,661.6
3c	0.86X + - 1.86	0.79	135.76 ^{ab}	93.06–252.34
3d	0.86X + - 1.86	1.11	119.22 ^a	85.21–198.87
3e	0.86X + - 2.26	0.34	400.44 ^{a-e}	221.7–1298.64
3f	0.893X + - 2.643	0.73	1088.69 ^{ef}	461.57–7540.64
3g	0.86X + - 2.46	1.60	1122.79 ^{d-f}	452.49–9494.94
3h	0.86X + - 2.26	0.34	532.89 ^{a-e}	259.81–2618.13
3i	0.571X + - 1.771	0.16	1174.88 ^{b-e}	387.61–32,677.63
3j	0.71X + - 1.91	0.29	535.24 ^{a-e}	255.58–2889.14
3k	0.71X + - 1.91	0.24	615.33 ^{a-e}	266.31–5112.63
3l	0.71X + - 1.71	0.23	319.15 ^{a-c}	169.51–1319.40
3m	1.071X + - 3.321	1.18	1674.03 ^{ef}	599.19–21,776.24
3n	1.0X + - 3.2	1.36	1260.7 ^{ef}	517.01–9960.98
3o	1.286X + - 3.886	0.53	1052.59 ^f	494.08–5622.39

* Carbendazim 50% WP, ED₅₀ = 9.132 $\mu\text{g mL}^{-1}$ * ED₅₀ values with different superscripts are significantly different ($p < 0.001$)

against *R. solani*, followed by **3j** (ED₅₀ = 2.28 $\mu\text{g mL}^{-1}$), **3g** (ED₅₀ = 4.35 $\mu\text{g mL}^{-1}$) and **3k** (ED₅₀ = 6.75 $\mu\text{g mL}^{-1}$) (Fig. 1). However, in case of *F. oxysporum* bioassay, compound **3d** (ED₅₀ = 119.22 $\mu\text{g mL}^{-1}$) showed highest

activity followed by **3c** (ED₅₀ = 135.76 $\mu\text{g mL}^{-1}$), **3l** (ED₅₀ = 319.15) and **3a** (ED₅₀ = 361.62 $\mu\text{g mL}^{-1}$) as compared to positive control, Carbendazim 50% WP (ED₅₀ = 9.01 $\mu\text{g mL}^{-1}$) (Fig. 2).

Structure activity relationship (SAR)

A series of imidazolylchalcones (3a–3o) with various substitutions on the benzaldehyde ring was synthesized to determine the structural requirements for their antifungal activity. Different substituents exhibited varying effects against both fungal species. For example, bromo derivatives (3c & 3d) showed higher activity, with mean ED₅₀ values of 8.64 mg L⁻¹ against *R. solani* and 127.49 mg L⁻¹ against *F. oxysporum*. In contrast, chloro derivatives (3j & 3l) were less effective than bromo, with mean ED₅₀ values of 15.77 mg L⁻¹ against *R. solani* and 427.19 mg L⁻¹ against *F. oxysporum* (Fig. 3).

Among chloro derivatives, monochloro derivatives (3j & 3l), having mean ED₅₀ values of 15.77 mg L⁻¹ against *R. solani* and 427.19 mg L⁻¹ against *F. oxysporum*, showed greater antifungal activity against both the fungi, as compared to dichloro derivatives (3a & 3k) with mean ED₅₀ values of 208.52 mg L⁻¹ against *R. solani* and 488.47 mg L⁻¹ against *F. oxysporum* (Fig. 4).

The compound with a single methoxy group (3i) exhibited greater antifungal potency against *R. solani* (ED₅₀ = 15.33 mg L⁻¹) compared to the compound with three methoxy groups (3o, 3,4,5-OMe), which had an ED₅₀ of 22.66 mg L⁻¹. However, 3o (ED₅₀ = 1052.59 mg L⁻¹) demonstrated higher antifungal activity against *F. oxysporum* than 3i (ED₅₀ = 1174.88 mg L⁻¹) (Fig. 5).

Among the nitro-substituted imidazolylchalcones (3e, 3f, and 3g), compound 3e (2-NO₂) exhibited the highest antifungal activity, with ED₅₀ values of 14.84 mg L⁻¹ against *R. solani* and 400.44 mg L⁻¹ against *F. oxysporum*. (Fig. 6).

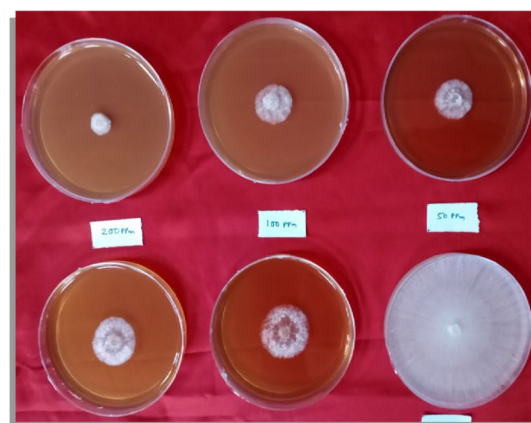
Other substituent introduced in the ring B like fluoro, hydroxyl and benzyloxy groups showed good to moderate antifungal activities. Finally, on comparing the mean ED₅₀ values of all the synthesized compounds against both fungi, we found that the compounds were generally more effective against *R. solani* (mean ED₅₀ 60.22 mg L⁻¹) compared to *F. oxysporum* (mean ED₅₀ 777.70 mg L⁻¹) (Fig. 7).

Nematicidal activity

The results of in vitro nematicidal activity of synthesized imidazolylchalcones against *M. incognita* (root knot nematode) are presented in Table 5, which revealed that compound **3f** (LC₅₀ = 33.62 $\mu\text{g mL}^{-1}$) showed highest activity followed by **3c** (LC₅₀ = 34.75 $\mu\text{g mL}^{-1}$), **3e** (LC₅₀ = 64.79 $\mu\text{g mL}^{-1}$) and **3l** (LC₅₀ = 69.11 $\mu\text{g mL}^{-1}$)

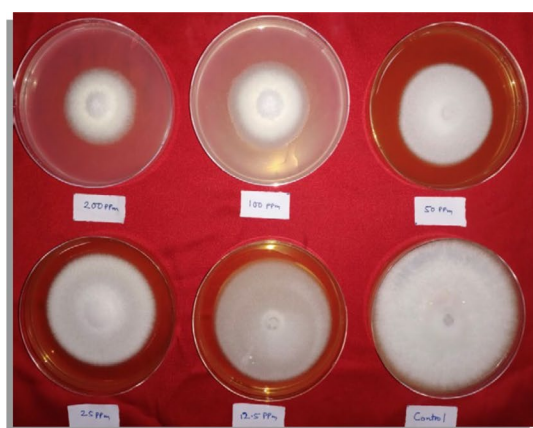


3h

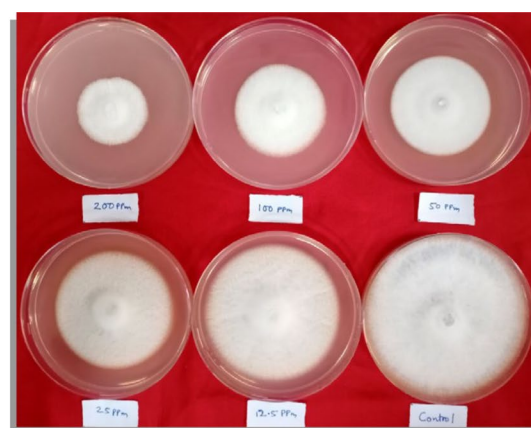


3j

Fig. 1 Fungicidal activity of potent molecules, **3h** and **3j** against *Rhizoctinia solani*



3c



3d

Fig. 2 Fungicidal activity of **3c** and **3d** against *Fusarium oxysporum*

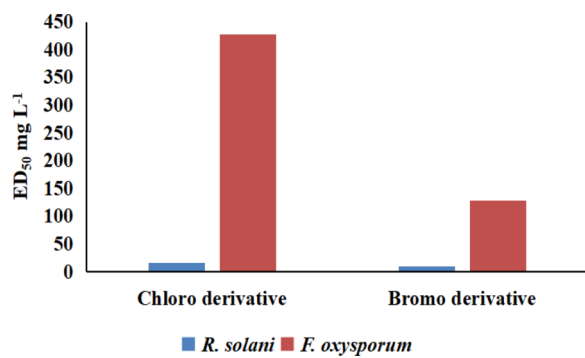


Fig. 3 Effect of chloro and bromo substituents on antifungal activity

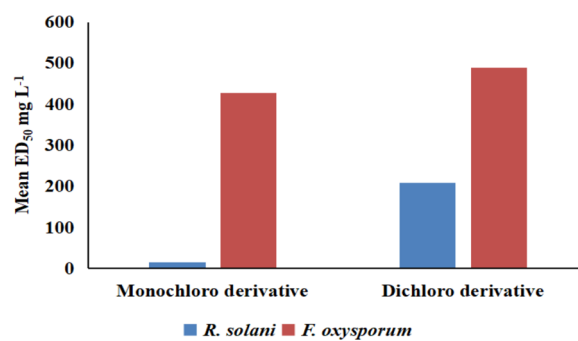


Fig. 4 Effect of chloro substituents on antifungal activity

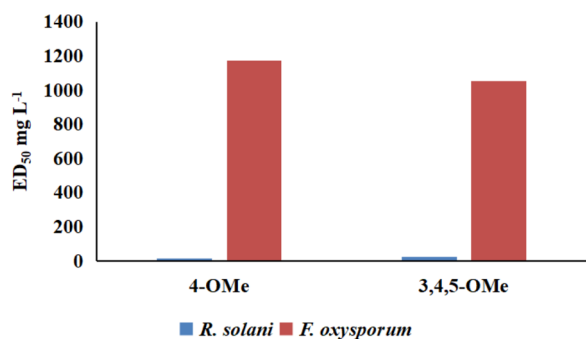


Fig. 5 Effect of methoxy substituents on antifungal activity

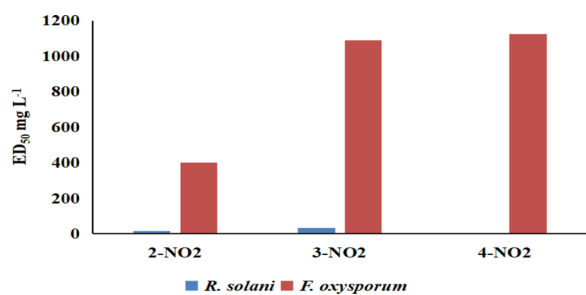


Fig. 6 Effect of nitro substituents on antifungal activity

after 24 h observation as compared to positive control Velum Prime 34.48% SC (Fluopyrum; LC₅₀ = 3.46 μg mL⁻¹).

Molecular docking

Molecular docking is a computational technique that enables virtual exploration of the interactions between proteins and molecules. This method plays a crucial role in the rational design, optimization, and characterization of protein–ligand interactions, contributing to the development of novel agrochemicals. In this study, molecular docking was employed to investigate the binding interactions of selected compounds with key target sites in two pathogenic fungi, *Sclerotium rolsii* and *Fusarium oxysporum*, as well as in the nematode *Meloidogyne incognita*. The study focused on two primary fungal targets: cutinase and elongation factor. Cutinases, hydrolytic enzymes found in fungal cell walls, catalyze the breakdown of glycosidic bonds in chitin. These enzymes play a pivotal role in facilitating fungal penetration into plant root tissues, enabling pathogens like *F. oxysporum* to establish primary infections. Due to its critical role in the pathogenic mechanism of *F. oxysporum*, cutinase represents an attractive target for antifungal intervention, potentially disrupting the fungus's ability to cause disease. Similarly, elongation factors, essential for fungal growth and survival, present another prime target for the development of fungicidal compounds [32, 54, 55]. Additionally, acetylcholinesterase, a vital enzyme for the regulation of nerve signal transmission, was explored as a target in *M. incognita*. This enzyme's crucial role in maintaining steady nerve signal transfer makes it an important target for pest control strategies against nematodes [56, 57]. These docking studies provide valuable insights into the molecular interactions at these target sites,

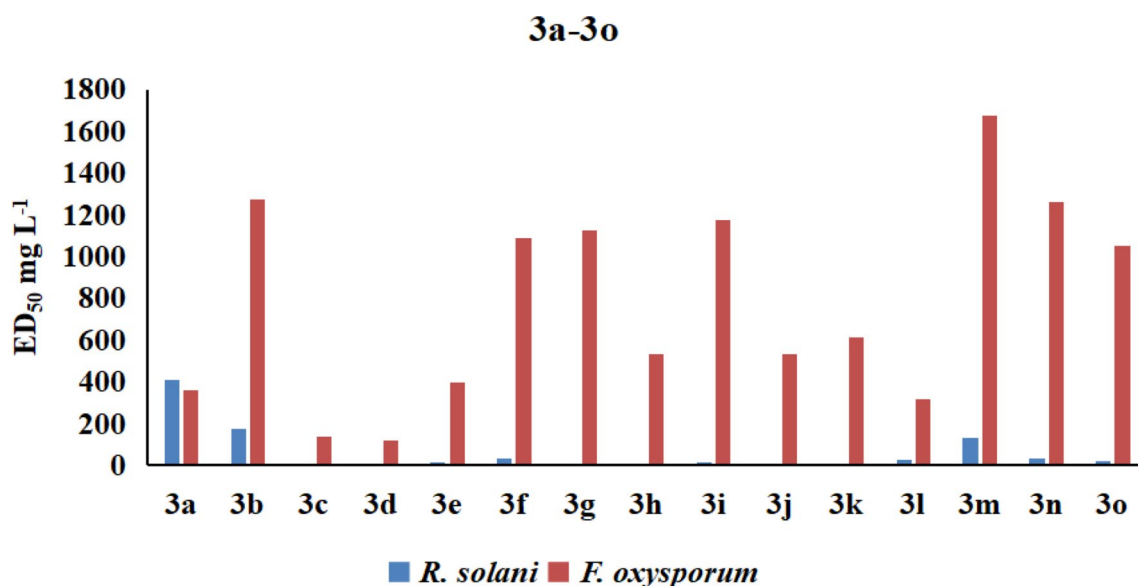


Fig. 7 Comparative analysis of the mean ED₅₀ values of 3a–3o

Table 5 Nematicidal activity of imidazolylchalcone derivatives against *Meloidogyne incognita*

Compounds	LC ₅₀ (µg mL ⁻¹)			
	24 h	48 h	72 h	96 h
3a	84.0 ^{ab}	77.15 ^e	70.49 ^f	66.43 ^d
3b	87.76 ^{ab}	82.52 ^d	77.93 ^d	68.99 ^c
3c	34.75 ^b	25.98 ⁱ	24.09 ^k	23.46 ^j
3d	87.19 ^{ab}	83.55 ^d	72.60 ^e	59.65 ^e
3e	64.79 ^{ab}	59.25 ^{fg}	53.93 ^g	47.53 ^g
3f	33.62 ^b	24.27 ⁱ	21.29 ^j	19.49 ^j
3g	90.13 ^{ab}	82.8 ^d	72.45 ^e	58.32 ^e
3h	133.22 ^a	122.9 ^b	96.11 ^b	77.65 ^b
3i	141.63 ^a	114.64 ^c	92.50 ^c	75.27 ^b
3j	195.84 ^{ab}	128.47 ^a	104.98 ^a	81.88 ^a
3k	84.95 ^b	60.79 ^f	43.55 ^h	32.06 ^h
3l	69.11 ^b	50.10 ^h	38.14 ^j	30.50 ^h
3m	78.05 ^b	55.85 ^g	41.08 ⁱ	29.74 ^h
3n	85.77 ^b	56.99 ^g	40.49 ^j	29.55 ^h
3o	172.89 ^{ab}	123.69 ^b	77.92 ^d	53.87 ^f

* Fluopyram (Velum) LC₅₀: 3.46 (24 h), 1.99 (48 h), 0.14 (72 h), 0.05 (96 h) µg mL⁻¹ (hr means hour)

* LC₅₀ values with different superscripts are significantly different (p < 0.001)

facilitating the design of effective antifungal and nematicidal agents.

The compound under study showed promising interactions with their respective target enzymes, as summarized in Table 6. The compound **3d** showing the best activity against *F. oxysporum*, strongly inhibited the activity of cutinase enzyme through conventional H bonding, C-H hydrogen bonding and π-Cation interactions involving the residues like ARG 102, ASN 427 and GLN 424; which was further stabilized by hydrophobic interaction such as π-Alkyl interactions involving ARG 425, ARG 380 and ARG 276. The compound **3h** was found to inhibit both the elongation factor and cutinase of *R. solani* strongly, however, the binding with elongation factor was stronger ($\Delta G = -9.7$ kcal/mol) as compared to cutinase ($\Delta G = -8.3$ kcal/mol). This bonding was again attributed towards the conventional hydrogen bond and π-Anion bond, further strengthened by hydrophobic interactions such as π-Alkyl, π-σ, and π-π T shaped interactions. The benzyloxy substitution in the benzaldehyde ring was found to be crucial in this regard as it formed hydrogen bond with LEU 77. Similarly, the compound **3f** was found to

Table 6 Binding energies of synthesized compounds against various target sites

Compound	Binding affinity (kcal/mol)					
	<i>Fusarium oxysporum</i>		<i>Rhizoctonia solani</i>		<i>Meloidogyne incognita</i>	
	Cutinase	Elongation factor	Cutinase	Elongation factor	Acetylcholinesterase	
3a	-8.3	-6.9	-7.5	-9.0	-9.7	
3b	-8.0	-6.8	-7.8	-9.0	-9.5	
3c	-8.3	-6.7	-7.2	-9.1	-8.8	
3d	-8.1	-6.9	-7.4	-9.2	-9.5	
3e	-8.7	-7.4	-7.6	-9.1	-9.6	
3f	-8.7	-7.3	-7.8	-9.4	-9.7	
3g	-8.6	-6.9	-7.7	-9.2	-8.9	
3h	-9.3	-6.5	-8.3	-9.7	-9.7	
3i	-8.1	-6.5	-7.4	-9.0	-8.6	
3j	-8.2	-6.9	-7.6	-8.8	-9.5	
3k	-8.5	-7.1	-7.9	-9.3	-9.5	
3l	-8.0	-7.1	-7.5	-9.2	-9.6	
3m	-8.3	-6.9	-7.5	-9.0	-9.4	
3n	-7.9	-6.9	-7.6	-8.9	-9.3	
3o	-8.2	-6.4	-7.1	-8.2	-8.7	
Positive control	-6.7	-5.5	-5.5	-6.9	-10.1	
	Carbendazim		Hexaconazole		Fluopyrum	

bind favorably with acetylcholinesterase of *M. incognita*. Conventional hydrogen bond involving SER 252 and HIS 514, along with some hydrophobic interactions such as π - π stacked, π - σ , and π - π T shaped interactions, helped in the binding process. Nitrophenyl substitution favored the formation of both the hydrogen bonds, resulting in stronger binding of the compound. Some discrepancies were observed between the molecular docking results and the outcomes of the in vitro experiments. Notably, while the compound **3d** demonstrated the most potent fungicidal activity

against *Fusarium oxysporum* in vitro, the in silico studies ranked it below compound **3h**, which exhibited the highest binding affinity. This divergence can be attributed to the inherent complexities of biological systems in vitro, which involve numerous interacting components, dynamic signaling pathways, and environmental fluctuations that are not fully accounted for in computational models. Furthermore, in actual biological environments, additional binding sites on the target molecule may become accessible, leading to

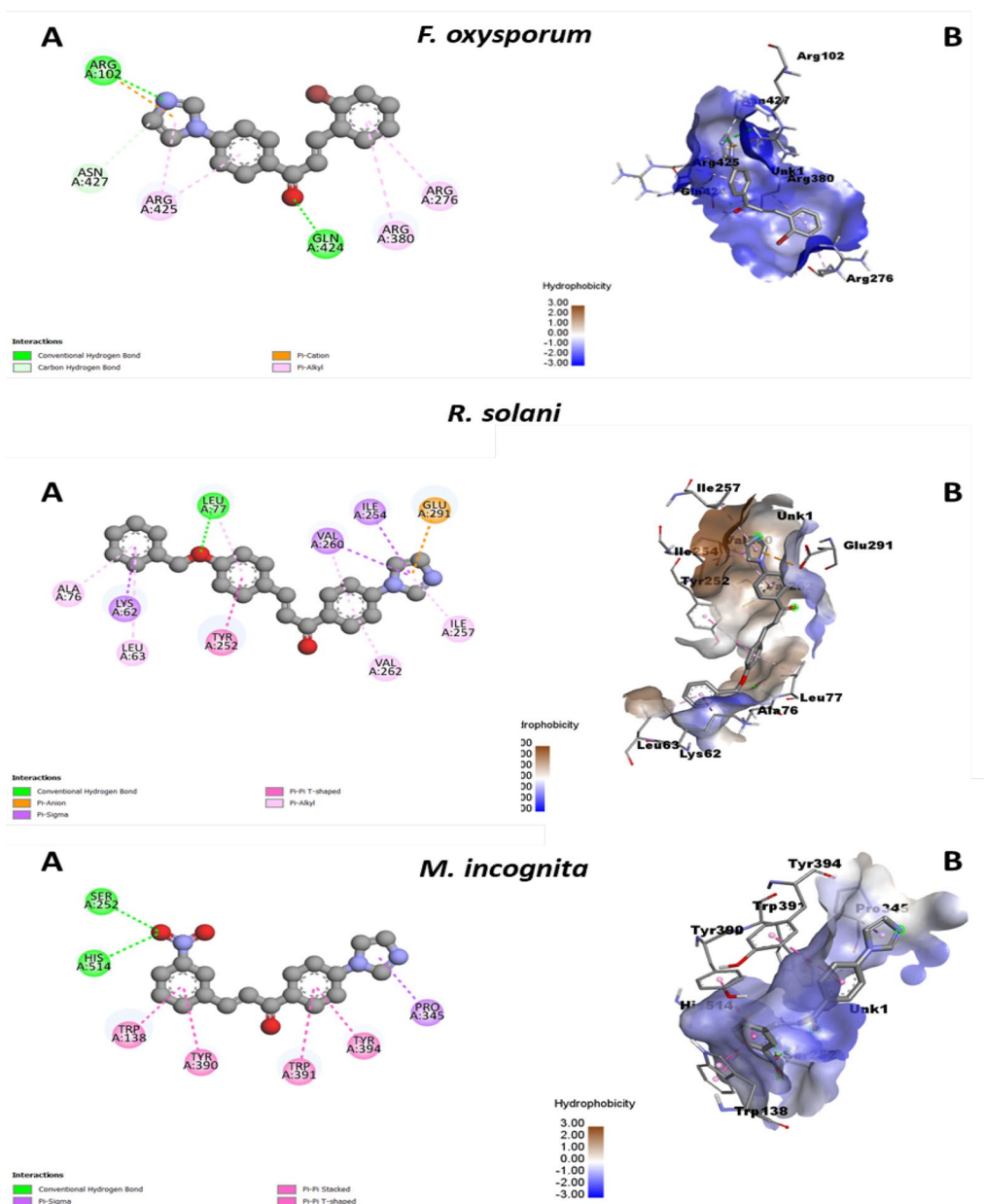


Fig. 8 2D interaction (A) and protein ligand binding (B) of **3d**, **3h**, and **3f** with their respective target sites of *F. oxysporum*, *R. solani*, and *M. incognita*

interactions that are not predicted by in silico docking analyses [58]. (Fig. 8).

Conclusion

This study presents synthesis of imidazolylchalcone derivatives via ultrasonication, a green method yielding higher efficiency in less time than conventional approaches. The compounds were characterized using spectroscopic techniques ($^1\text{H-NMR}$, $^{13}\text{C-NMR}$, HRMS) and evaluated for antifungal and nematocidal activities. Compound 3h ($\text{ED}_{50}=0.69 \mu\text{g/mL}$) showed superior efficacy against *R. solani* compared to commercial hexaconazole ($\text{ED}_{50}=3.75 \mu\text{g/mL}$), while compound 3d ($\text{ED}_{50}=119.22 \mu\text{g/mL}$) was most effective against *E. oxysporum* but less effective than carbendazim. In nematocidal assays, compound 3f ($\text{LC}_{50}=33.62 \mu\text{g/mL}$) exhibited activity against *M. incognita* but was less potent than Velum Prime. Moreover, these compounds are having highly electronegative atoms, which make strong hydrogen bonding with enzymes active site and activate phenyl rings. Furthermore, molecular docking confirmed strong enzyme binding with active site of targeted enzyme. The potent compound/s in this series could serve as lead compounds for the development of effective antifungal and antinematic agents with appropriate formulation to control soil-borne diseases.

Supplementary Information

The online version contains supplementary material available at <https://doi.org/10.1186/s13065-025-01451-z>.

Supplementary file 1: Supporting information includes chemical structure, $^1\text{H-NMR}$, $^{13}\text{C-NMR}$ and HRMS spectra of most effective compounds 3d, 3f and 3h with 3a as representative of imidazolylchalcone derivatives. $^1\text{H-NMR}$ and $^{13}\text{C-NMR}$ of all synthesized compounds.

Acknowledgements

The authors gratefully acknowledge ICAR-Indian Agricultural Research Institute for providing facilities to carry out the research work and thankful for the financial support received from DST, PI Industries Ltd., CII, New Delhi and Prime Minister's Fellowship for financial support.

Author contributions

RK: design of the work, acquisition, analysis, interpretation of data and drafted work KPT: analysis, interpretation of data PK: design of the work, substantively revised RG: interpretation of data and drafted work SRM: analysis and draft revision VK: experimentation, draft revision PCM: analysis and interpretation of data J: experimentation and drafting VSR: design of the work, interpretation of data P: analysis, interpretation of data VS: interpretation of data DK: substantively revised draft NAS: conceptualize, supervision, design of the work, interpretation of data.

Funding

Financial support received from PI Industries Ltd. And CII, New Delhi as Prime Minister's Fellowship and other facility support from ICAR- Indian Agricultural Research Institute, New Delhi-110012.

Availability of data and materials

The data generated and/or analyzed during the current study are not publicly available due feasibility of the study to begin a further in-vivo trial; however, they are available from the corresponding author upon reasonable request.

Declarations

Ethics approval and consent to participate

The research proposal including the use of fungi and nematodes was approved by the Institute Research Committee, 2020 under the chairmanship of the Director, Joint Director & Dean and Head of the Division of Agricultural Chemicals, ICAR-Indian Agricultural Research Institute, New Delhi (ID_11375). The research was conducted in accordance with the ethical standards of the institutional and/or national research committee.

Consent for publication

Not applicable.

Competing interests

The authors declare no competing interests.

Author details

¹Division of Agricultural Chemicals, ICAR-Indian Agricultural Research Institute, New Delhi, India. ²The Graduate School, ICAR-Indian Agricultural Research Institute, New Delhi, India. ³ICAR-Central Inland Fisheries Research Institute, RC, Guwahati, Assam, India. ⁴ICAR- National Research Centre on Seed Spices, Ajmer, Rajasthan, India. ⁵Division of Nematology, ICAR-Indian Agricultural Research Institute, New Delhi, India. ⁶Division of Plant Pathology, ICAR-Indian Agricultural Research Institute, New Delhi, India. ⁷PI Industries, Udaipur, India.

Received: 10 January 2025 Accepted: 11 March 2025

Published online: 29 April 2025

References

- Oraon S, Padamini R, Shahni YS, Das N, Sinha D, Sujatha GS, Singh OB, Karanwal R. Impact of emerging pathogens in crop production. *Microbiol Res J Int.* 2024;34(7):80–92.
- Khan MR, Ahamad I, Shah MH. Emerging important nematode problems in field crops and their management. In: Singh KP, Jahagirdar S, Sarma BK, editors. *Emerging trends in plant pathology*. Singapore: Springer; 2021. p. 33–62.
- Hassan MA, Pham TH, Shi H, Zheng J. Nematodes threats to global food security. *Acta Agric Scand Sect B-Soil Plant Sci.* 2013;63(5):420–5.
- Keatinge JDH, Yang RY, Hughes JDA, Easdown WJ, Holmer R. The importance of vegetables in ensuring both food and nutritional security in attainment of the Millennium Development Goals. *J Food Secur.* 2011;3(4):491–501. <https://doi.org/10.1007/s12571-011-0150-3>.
- El-Kazzaz MK, Ghoneim KE, Agha MKM, Helmy A, Behiry SI, Abdelkhalik A, Saleem MH, Al-Askar AA, Arishi AA, Elsharkawy MM. Suppression of pepper root rot and wilt diseases caused by *Rhizoctonia solani* and *Fusarium oxysporum*. *Life.* 2022;12(4):587.
- Bhatti KH, Kausar N, Rashid U, Hussain K, Nawaz K, Siddiqi EH. Effects of biotic stresses on eggplant (*Solanum melongena* L.). *World Appl Sci J.* 2013;26(3):302–11. <https://doi.org/10.5829/idosi.wasj.2013.26.03.13460>.
- Kaniyassery A, Thorat SA, Kiran KR, Murali TS, Muthusamy A. Fungal diseases of eggplant (*Solanum melongena* L.) and components of the disease triangle: a review. *J Crop Improv.* 2023;37(4):543–94. <https://doi.org/10.1080/15427528.2022.2120145>.
- Singh BK, Singh SSBK, Yadav SM. Some important plant pathogenic disease of brinjal (*Solanum melongena* L.) and their management. *Plant Pathol J.* 2014;13(3):208–13.
- Gupta VK, Paul YS. Fungal diseases of tomato, chilli and brinjal. In: *Diseases of Vegetable Crops*. Kalyani Publishers; Ludhiana. 2001.
- Gawade BH, Chaturvedi S, Khan Z, Pandey CD, Gangopadhyay KK, Dubey SC, Chalam VC. Evaluation of brinjal germplasm against root-knot nematode, *Meloidogyne incognita*. *Indian Phytopathol.* 2022;75(2):449–56.
- Kumar R, Kundu A, Dutta A, Saha S, Das A, Bhowmik A. Chemo-profiling of bioactive metabolites from *Chaetomium globosum* for biocontrol of

- Sclerotinia rot and plant growth promotion. *Fungal Biol.* 2021;125(3):167–76. <https://doi.org/10.1016/j.funbio.2020.07.009>.
12. Ul Haq I, Sarwar MK, Faraz A, Latif MZ. Synthetic chemicals: major component of plant disease management. In: Ul Haq I, Ijaz S, editors. *Plant disease management strategies for sustainable agriculture through traditional and modern approaches*. Cham: Springer; 2020. p. 53–81.
 13. DeVito SC. On the design of safer chemicals: a path forward. *Green Chem.* 2016;18(16):4332–47. <https://doi.org/10.1039/C6GC00526H>.
 14. Shamim S, Khan KM, Ali M, Mahdavi M, Salar U, Mohammadi-Khanaposthani M, Faramarzi MA, Ullah N, Taha M. Diphenyl-substituted triazine derivatives: synthesis, α -glucosidase inhibitory activity, kinetics and in silico studies. *Future Med Chem.* 2023;15(18):1651–68. <https://doi.org/10.4155/fmc-2023-0057>.
 15. Khan S, Hussain R, Khan Y, Iqbal T, Khan MB, Al-Ahmary KM, Al Mhyawi SR. Insight into role of triazole derived Schiff base bearing sulfonamide derivatives in targeting Alzheimer's disease: synthesis, characterization, in vitro and in silico assessment. *J Mol Struct.* 2024. <https://doi.org/10.1016/j.molstruc.2024.138845>.
 16. Khan S, Hussain R, Ullah H, Khan Y, Iqbal T, Anwar S, Iqbal R, Khan IU, Almoallim HS, Ansari MJ. Identification of 1, 2, 4-triazole-bearing Bis-Schiff base hybrid scaffolds: in vitro and in silico insights to develop promising anti-urease and anti-cancer agents. *Results Chem.* 2024;7:101540. <https://doi.org/10.1016/j.rechem.2024.101540>.
 17. Yuan Y, Li M, Apostolopoulos V, Matsoukas J, Wolf WM, Blaskovich MA, Bojarska J, Ziora ZM. Tetrazoles: a multi-potent motif in drug design. *Eur J Med Chem.* 2024. <https://doi.org/10.1016/j.ejmech.2024.116870>.
 18. Hussain R, Khan S, Ullah H, Ali F, Khan Y, Sardar A, Iqbal R, Ataya FS, El-Sabbagh NM, Batiha GES. Benzimidazole-based schiff base hybrid scaffolds: a promising approach to develop multi-target drugs for alzheimer's disease. *Pharm.* 2023;16(9):1278. <https://doi.org/10.3390/ph16091278>.
 19. Hussain R, Rehman W, Rahim F, Khan S, Alanazi AS, Alanazi MM, Rasheed L, Khan Y, Shah SAA, Taha M. Synthesis, in vitro thymidine phosphorylase inhibitory activity and molecular docking study of novel pyridine-derived bis-oxadiazole bearing bis-schiff base derivatives. *Arab J Chem.* 2023;16(6):104773. <https://doi.org/10.1016/j.arabjc.2023.104773>.
 20. Iqbal T, Khan S, Rahim F, Tayyab M, Hussain R, Khan Y, Fiaz Z, Bibi S, Ullah H, Alzahran AYA, Alraih AM. Insights into the role of potent thiazidiazole based Schiff base derivatives in targeting type-II diabetes: a combine in-vitro and in-silico approaches. *J Mol Struct.* 2025;1321:140000. <https://doi.org/10.1016/j.molstruc.2024.140000>.
 21. Khan S, Iqbal T, Khan MB, Hussain R, Khan Y, Darwish HW. Novel pyrrole based triazole moiety as therapeutic hybrid: synthesis, characterization and anti-Alzheimer potential with molecular mechanism of protein ligand profile. *BMC Chem.* 2024;18(1):223. <https://doi.org/10.1186/s13065-024-01340-x>.
 22. Khan Y, Maalik A, Rehman W, Alanazi MM, Khan S, Hussain R, Rasheed L, Saboor A, Iqbal S. Synthesis, in vitro bio-evaluation and in silico molecular docking studies of thiazidiazole-based Schiff base derivatives. *Future Med Chem.* 2024;16(4):335–48. <https://doi.org/10.4155/fmc-2023-0276>.
 23. Khan S, Ullah H, Hussain R, Khan Y, Khan MU, Khan M, Sattar A, Khan MS. Synthesis, in vitro bio-evaluation, and molecular docking study of thiosemicarbazone-based isatin/bis-Schiff base hybrid analogues as effective cholinesterase inhibitors. *J Mol Struct.* 2023;1284:135351. <https://doi.org/10.1016/j.molstruc.2023.135351>.
 24. Poyraz S, Yildirim M, Ersatir M. Recent pharmacological insights about imidazole hybrids: a comprehensive review. *Med Chem Res.* 2024. <https://doi.org/10.1007/s00044-024-03230-2>.
 25. Khan S, Iqbal T, Mehmood T, Hussain R, Khan Y, Iqbal J, Ahmad Z, Darwish HW. Biological study with molecular mechanism of imidazo-thiazole based Schiff bases as anti-Alzheimer agent: Insight into the role of synthesis, molecular docking and ADMET analysis. *J Mol Struct.* 2025;1321:139995. <https://doi.org/10.1016/j.molstruc.2024.139995>.
 26. Arif S, Khan S, Iqbal T, Yallur BC, Rahim F, Hussain R, Khan Y, Ullah H. Synthesis, characterization, DFT, ADMET and molecular docking reveals the binding mechanism of hydroxyl containing bis-Schiff base derivatives: an approach toward Alzheimer disease. *Results Chem.* 2024;10:101706. <https://doi.org/10.1016/j.rechem.2024.101706>.
 27. Abbasi SA, Rehman W, Rahim F, Hussain R, Hawsawi MB, Alluhaibi MS, Alharbi M, Taha M, Khan S, Rasheed L, Wadood A. Molecular modeling and synthesis of novel benzimidazole-derived thiazolidinone bearing chalcone derivatives: a promising approach to develop potential anti-diabetic agents. *Z Naturforsch.* 2024. <https://doi.org/10.1515/znc-2024-0202>.
 28. Shakil NA, Singh MK, Kumar J, Sathiyendiran M, Kumar G, Singh MK, Pandey RP, Pandey A, Parmar VS. Microwave synthesis and antifungal evaluations of some chalcones and their derived diaryl-cyclohexenones. *J Environ Sci Health B.* 2010;45(6):524–30. <https://doi.org/10.1080/03601234.2010.493482>.
 29. Shakil NA, Singh MK, Sathiyendiran M, Kumar J. Microwave accelerated solvent-free synthesis and antifungal evaluations of flavanones. *Arch Phytopathol Pflanzenschutz.* 2011;44(20):1958–65. <https://doi.org/10.1080/03235408.2010.544467>.
 30. Shakil NA, Singh MK, Sathiyendiran M, Kumar J, Padaria JC. Microwave synthesis, characterization and bio-efficacy evaluation of novel chalcone based 6-carboxy-2-cyclohexen-1-one and 2H-indazol-3-ol derivatives. *Eur J Med Chem.* 2013;59:120–31. <https://doi.org/10.1016/j.ejmech.2012.10.038>.
 31. Yadav DK, Kaushik P, Pankaj, Rana VS, Kamil D, Khatri D, Shakil NA. Microwave assisted synthesis, characterization and biological activities of ferrocenyl chalcones and their QSAR analysis. *Front Chem.* 2019;7:814. <https://doi.org/10.3389/fchem.2019.00814>.
 32. Godara R, Kaushik P, Tripathi K, Kumar R, Rana VS, Kumar R, Mandal A, Shanmugam V, Pankaj, Shakil NA. Green synthesis, structure–activity relationships, in silico molecular docking, and antifungal activities of novel prenylated chalcones. *Front Chem.* 2024;12:1389848. <https://doi.org/10.3389/fchem.2024.1389848>.
 33. Gogiseti G, Kanna U, Sharma V, Rao Allaka T, Rao Tadiboina B. Design, synthesis and bio-evaluation of novel chalcones bridged with 1, 3, 4-oxadiazole linkers: ADMET and docking analysis. *Chem Biodivers.* 2022;19(12):202200681. <https://doi.org/10.1002/cbdv.202200681>.
 34. Sadineni K, Reddy Basireddy S, Rao Allaka T, Yatam S, Bhoomandla S, Muvvala V, Babu Haridasyam S. Design, synthesis and in vitro antitubercular effect of new chalcone derivatives coupled with 1, 2, 3-triazoles: a computational docking techniques. *Chem Biodivers.* 2024;21(5):202400389. <https://doi.org/10.1002/cbdv.202400389>.
 35. Siwach A, Verma PK. Synthesis and therapeutic potential of imidazole containing compounds. *BMC chem.* 2021;15:1–69.
 36. Rani N, Sharma A, Kumar Gupta G, Singh R. Imidazoles as potential anti-fungal agents: a review. *Mini Rev Med Chem.* 2013;13(11):1626–55.
 37. Reddy AB, Allaka TR, Avuthu VSR, Kishore PV, Nagarajaiah H. Imidazole-oxadiazole hybrid as potential antimicrobial agents: design, synthesis, drug-likeness, pharmacophore and molecular docking study. *ChemistrySelect.* 2024;9(32):202401989. <https://doi.org/10.1002/slct.202401989>.
 38. Shaik KM, Pandurangan K, Allaka TR, Ahmed MZ, Gunda SK. Synthesis and biological evaluation of novel benzo [d] imidazole bearing oxadiazolyl-triazole derivatives as potential anticancer agents: a computational docking technique. *Next Res.* 2025;2(1):100145. <https://doi.org/10.1016/j.nexres.2025.100145>.
 39. Tolomeu HV, Fraga CAM. Imidazole: synthesis, functionalization and physicochemical properties of a privileged structure in medicinal chemistry. *Molecules.* 2023;28(2):838.
 40. Banerjee B. Recent developments on ultrasound assisted catalyst-free organic synthesis. *Ultrason Sonochem.* 2017;35:1–14. <https://doi.org/10.1016/j.jultsonch.2016.09.023>.
 41. Karmakar R, Mukhopadhyay C. Ultrasonication under catalyst-free condition: an advanced synthetic technique toward the green synthesis of bioactive heterocycles. In: Brahmachari G, editor. *Green synthetic approaches for biologically relevant heterocycles*. Amsterdam: Elsevier; 2021. p. 497–562.
 42. Puri S, Kaur B, Parmar A, Kumar H. Applications of ultrasound in organic synthesis—a green approach. *Curr Org Chem.* 2013;17(16):1790–828.
 43. Mason TJ. Ultrasound in synthetic organic chemistry. *Chem Soc Rev.* 1997;26(6):443–51. <https://doi.org/10.1039/CS9972600443>.
 44. Suslick KS, Hammerton DA, Cline RE. Sonochemical hot spot. *J Am Chem Soc.* 1986;108(18):5641–2. <https://doi.org/10.1021/ja00278a055>.
 45. Liu YT, Sun XM, Yin DW, Yuan F. Syntheses and biological activity of chalcones-imidazole derivatives. *Res Chem Inter.* 2013;39(3):1037–48.
 46. Nene YL, Thapliyal PN. Fungicides in plant disease control. In: Nene YL, Thapliyal PN, editors. *Evaluation of fungicides*. New Delhi: Oxford and IBH Publishing Co.; 1979. p. 406–28.

47. Kaushik P, Shakil NA, Rana VS. Synthesis, biological evaluation, and QSAR studies of 3-iodochromone derivatives as potential fungicides. *Front Chem.* 2021;9:636882. <https://doi.org/10.3389/fchem.2021.636882>.
48. Abbott WS. A method of computing the effectiveness of an insecticide. *J Econ Entomol.* 1925;18(2):265–7.
49. Kumar V, Mondal PC, Kumar R, Kaushik P, Shakil NA, Gowda AA, Rana VS. Composition and nematicidal activity of the essential oil from *Piper longum* against root knot nematode. *Indian J Agric Sci.* 2023;93(7):774–9. <https://doi.org/10.56093/ijas.v93i7.135197>.
50. Yadav DK, Kaushik P, Tripathi KP, Rana VS, Yeasin M, Kamil D, Pankaj, Khatri D, Shakil NA. Bioefficacy evaluation of ferrocenyl chalcones against *Meloidogyne incognita* and *Sclerotium rolfsii* infestation in tomato. *J Environ Sci Health B.* 2022;57(3):192–200. <https://doi.org/10.1080/03601234.2022.2042154>.
51. Yadav DK, Tripathi KP, Pankaj P, Kaushik P, Rana VS, Khatri D, Shakil NA. Antinematic activity of ferrocenyl chalcones against *Meloidogyne incognita* infestation in tomato. *Indian J Agric Sci.* 2021;91(2):305–9. <https://doi.org/10.56093/ijas.v91i2.111644>.
52. Tripathi K, Kaushik P, Yadav DK, Kumar R, Misra SR, Godara R, Bashyal BM, Rana VS, Kumar R, Yadav J, Shakil NA. Synthesis, antifungal evaluation, two-dimensional quantitative structure–activity relationship and molecular docking studies of isoxazole derivatives as potential fungicides. *Pest Manag Sci.* 2024. <https://doi.org/10.1002/ps.8152>.
53. Lohning EA, Levonis MS, Williams-Noonan B, Schweiker SSA. practical guide to molecular docking and homology modelling for medicinal chemists. *Current Topics Med Chem.* 2017;17(18):2023–40.
54. Dimarogona M, Nikolaivits E, Kanelli M, Christakopoulos P, Sandgren M, Topakas E. Structural and functional studies of a *Fusarium oxysporum* cutinase with polyethylene terephthalate modification potential. *Biochim Biophys Acta (BBA)-General Subj.* 2015;1850(11):2308–17.
55. Taruna A, Dewi RR, Hadiwijoyo E, Yulianah I, Syib'li MA, Abadi AL. Molecular docking and in vitro study revealed the inhibition mechanism of Cutinase of *Fusarium oxysporum* f. sp. *lycopersici* by natural compounds of local turmeric in Indonesia. *AGRIVITA J Agric Sci.* 2023;45(3):554–69.
56. Mondal PC, Kumar V, Kaushik P, Shakil NA, Pankaj, Rana VS. New nematicidal compounds from *Mentha spicata* L. against *Meloidogyne incognita*. *J Plant Dis Prot.* 2024;131(6):1983–92.
57. Yadav N, Kumar R, Sangwan S, Dhanda V, Rani R, Devi S, Duhan A, Sindhu J, Chauhan S, Malik VK, Yadav S. Design, synthesis, nematicidal evaluation, and molecular docking study of pyrano [3, 2-c] pyridones against *Meloidogyne incognita*. *J Agric Food Chem.* 2024;72(28):15512–22.
58. Chen YC. Beware of docking! *Trends Pharmacol Sci.* 2015;36(2):78–95.

Publisher's Note

Springer Nature remains neutral with regard to jurisdictional claims in published maps and institutional affiliations.